1

Polymer Rheology by Dielectric Spectroscopy

Clement Riedel[1], Angel Alegria[1], Juan Colmenero[1] and Phillipe Tordjeman[2]
[1]*Universidad del Pais Vasco / Euskal Herriko Unibertsitatea*
[2]*Université de Toulouse, INPT*
[1]*Spain*
[2]*France*

1. Introduction

The aim of this chapter is to discuss the main models describing the polymer dynamics at macroscopic scale and present some of the experimental techniques that permit to test these models. We will notably show how Broadband Dielectric Spectroscopy (BDS) permits to obtain rheological information about polymers, i.e. permits to understand how the matter flows and moves. We will focus our study the whole chain motion of cis-polyisoprene 1,4 (PI).

Due to dipolar components both parallel and perpendicular to the chain backbone, PI exhibits a whole chain dielectric relaxation (normal mode) in addition to that associated with segmental motion. The Rouse model (Rouse, 1953), developed in the fifties, is well known to describe rather correctly the whole chain dynamics of unentangled polymers. In the past, the validity of the Rouse model has ever been instigated by means of different experimental techniques (BDS, rheology, neutron scattering) and also by molecular dynamics simulations. However this study is still challenging because in unentangled polymer the segmental dynamics contributions overlap significantly with the whole chain dynamics. In this chapter, we will demonstrate how we have been able to decorelate the effect of the α-relaxation on the normal mode in order to test how the Rouse model can quantitatively describes the normal mode measured by BDS and rheology. The introduction of polydispersity is a key point of this study.

The reptational tube theory, first introduced by de Gennes de Gennes (1979) and developed by Doi and Edwads Doi & Edwards (1988) describes the dynamics of entangled polymers where the Rouse model can not be applied. Many corrections (as Contour Length Fluctuation or Constraints Release) have been added to the pure reptation in order to reach a totally predictive theory McLeish (2002); Viovy et al. (2002). In the last part of this chapter, we will show how the relaxation time of the large chain dynamics depends on molecular weight and discuss the effects of entanglement predicted by de Gennes theory on dielectric spectra. PI is a canonical polymer to study the large chain dynamics; however, due to its very weak relaxation, the measurement of this dynamics at nanoscale is still challenging.

2. Material and methods

2.1 Polyisoprene samples

Polymers are characterized by a distribution of sizes known as polydispersity. Given a distribution of molecular sizes (N_i molecules of mass M_i), the number-averaged molecular weight M_n is defined as the first moment of distribution (Eq. 1) and the mass-averaged molecular weight M_w as the ratio between the second and first moments of the distribution (Eq. 2).

$$M_n = \sum_i \frac{N_i M_i}{N_i} \tag{1}$$

$$M_w = \sum_i \frac{N_i M_i^2}{N_i M_i} \tag{2}$$

The polydispersity I_p is the ratio Mw/Mn.

Polymers can have dipoles in the monomeric unit that can be decomposed in two different components: parallel or perpendicular to the chain backbone. The dipole moment parallel to the chain backbone giving rise to an "end-to-end" net polarization vector will induce the so-called dielectric normal mode dielectric relaxation that can be studied using theoretical models. The dipole moment perpendicular to the chain backbone will lead to the segmental α-relaxation that can only be described using empirical models, since no definitive theoritical framework exists for this universal process.

We have chosen to study the relaxations of two different samples. The first is 1,4-cis-polyisoprene (PI). This isomer is a A-type polymer in the Stockmayer classification Stockmayer (1967): it carries both local dipole moments parallel and perpendicular to the chain backbone. The chapter on the large scale dynamics will be focused on the study of the dynamics of the normal mode of PI.

The polyisoprene (PI) samples were obtained from anionic polymerization of isoprene (Fig. 1). According to the supplier, Polymer Source, the sample is linear (no ramification) and its micro-composition is 80% cis, 15% trans and 5% other 1. We are working with the isomer *cis* that have a net end-to-end polarization vector. Before the experiments samples were dried in a vacuum oven at 70 žC for 24 hours to remove any trace of solvent.

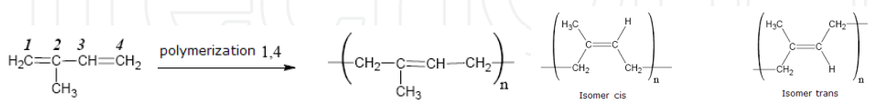

(a) Polymerization of isoprene (b) Isomer cis and trans

Fig. 1. Polymerization and isomer of isoprene

For our study, seven samples have been chosen to cover a large band of molecular weight with low polydispersity (Table 1). The polydispersity (determined from size-exclusion chromatography experiments) is given by supplier while the glass transition temperature (T_g) has been measured by differential scanning calorimetry. To avoid oxidation, PI samples were stored at -25 žC.

Sample	M_n [kg/mol]	M_w [kg/mol]	I_p	T_g [K]
PI-1	1.1	1.2	1.11	194
PI-3	2.7	2.9	1.06	203
PI-10	10.1	10.5	1.04	209
PI-33	33.5	34.5	1.04	210
PI-82	76.5	82	1.07	210
PI-145	138	145	1.07	210
PI-320	281	320	1.14	210

Table 1. Molecular weight, polydispersity and T_g of PI

2.2 Rheology

Elasticity is the ability of a material to store deformational energy, and can be viewed as the capacity of a material to regain its original shape after being deformed. Viscosity is a measure of the ability of a material to resist flow, and reflects dissipation of deformational energy through flow. Material will respond to an applied force by exhibiting either elastic or viscous behavior, or more commonly, a combination of both mechanisms. The combined behavior is termed viscoelasticity. In rheological measurements, the deformational force is expressed as the stress, or force per unit area. The degree of deformation applied to a material is called the strain. Strain may also be expressed as sample displacement (after deformation) relative to pre-deformation sample dimensions.

Dynamic mechanical testing involves the application of an oscillatory strain $\gamma(t) = \gamma_0 \, cos(\omega t)$ to a sample. The resulting sinusoidal stress $\sigma(t) = \sigma_0 \, cos(\omega t + \delta)$ is measured and correlated against the input strain, and the viscous and elastic properties of the sample are simultaneously measured.

If the sample behaves as an ideal elastic solid, then the resulting stress is proportional to the strain amplitude (Hooke's Law), and the stress and strain signals are in phase. The coefficient of proportionality is called the shear modulus G. $\sigma(t) = G \, \gamma_0 \, cos(\omega t)$ If the sample behaves as an ideal fluid, then the stress is proportional to the strain rate, or the first derivative of the strain (Newton's Law). In this case, the stress signal is out of phase with the strain, leading it by 90ř. The coefficient of proportionality is the viscosity η. $\sigma(t) = \eta \, \omega \, \gamma_0 \, cos(\omega t + \pi/2)$

For viscoelastic materials, the phase angle shift (δ) between stress and strain occurs somewhere between the elastic and viscous extremes. The stress signal generated by a viscoelastic material can be separated into two components: an elastic stress (σ') that is in phase with strain, and a viscous stress (σ'') that is in phase with the strain rate (dγ/dt) but 90ř out of phase with strain. The elastic and viscous stresses are sometimes referred to as the in-phase and out-of-phase stresses, respectively. The elastic stress is a measure of the degree to which the material behaves as an elastic solid. The viscous stress is a measure of the degree to which the material behaves as an ideal fluid. By separating the stress into these components, both strain amplitude and strain rate dependence of a material can be simultaneously measured. We can resume this paragraph by a set of equation:

$$\sigma(t) = \left(\frac{\sigma_0 \, cos(\delta)}{\gamma_0} \right) \gamma_0 \, cos(\omega \, t) + \left(\frac{\sigma_0 \, sin(\delta)}{\gamma_0} \right) \gamma_0 \, sin(\omega \, t) \tag{3}$$

$$G' = \frac{\sigma_0 \, cos(\delta)}{\gamma_0} \quad G'' = \frac{\sigma_0 \, cos(\delta)}{\gamma_0} \tag{4}$$

$$\underline{G}(\omega) = G' + iG'' \tag{5}$$

2.3 Broadband dielectric spectroscopy

The set-up of a broadband dielectric spectroscopy (BDS) experiment is displayed in Fig. 2. The sample is placed between two electrodes of a capacitor and polarized by a sinusoidal voltage $\underline{U}(\omega)$. The result of this phenomena is the orientation of dipoles which will create a capacitive system. The current $\underline{I}(\omega)$ due to the polarization is then measured between the electrode. The complex capacity $\underline{C}(\omega)$ of this system is describe by the complex dielectric function $\underline{\epsilon}(\omega)$ as:

$$\underline{\epsilon}(\omega) = \epsilon'(\omega) - i\,\epsilon''(\omega) = \frac{\underline{C}(\omega)}{C_0} = \frac{\underline{J}(\omega)}{i\,\omega\,\epsilon_0 \underline{E}(\omega)} = \frac{\underline{I}(\omega)}{i\,\omega\,\underline{U}(\omega)\,C_0} \tag{6}$$

where: C_0 is the vacuum capacitance of the arrangement

$\underline{E}(\omega)$ is the sinusoidal electric field applied (within the linear response)
$\underline{J}(\omega)$ is the complex current density $\epsilon_0 = 8.85\,10^{-12} A\,s\,V^{-1}\,m^{-1}$is the permittivity of vacuum

ϵ' and ϵ'' are proportional to the energy stored and lost in the sample, respectively.

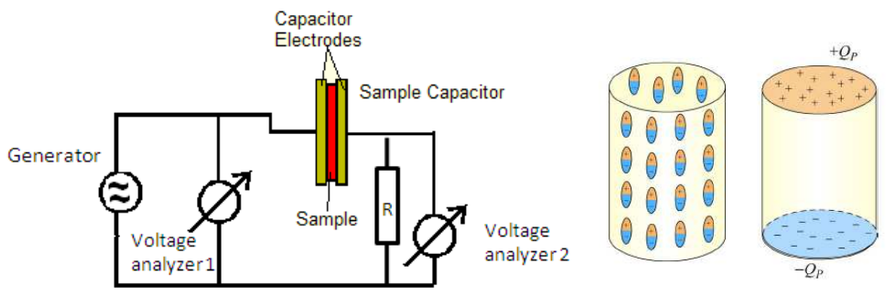

(a) Schema of the principle of BDS

(b) Polarization of matter and resulting capacitive system

Fig. 2. Schema of the principle of BDS and polaryzation of matter

In our experiments samples were placed between parallel gold-plated electrodes of 20 mm diameter and the value of the gap (between the electrodes) was fixed to 0.1mm (by a narrow PTFE cross shape piece).

Polarization of matter ($\overrightarrow{P}$) can be describe as damped harmonic oscillator. When the electromagnetic field is sinusoidal the dipole oscillates around its position of equilibrium. This response is characterized by $\underline{\epsilon}(\omega)$:

$$\overrightarrow{P} = (\underline{\epsilon}(\omega) - 1)\epsilon_0 \, \overrightarrow{E}\,(\omega) \tag{7}$$

The complex dielectric function is the one-sided Fourier or pure imaginary Laplace transform of the correlation function of the polarization fluctuations $\phi(t) = [\overrightarrow{P}\,(t) \cdot \overrightarrow{P}\,(0)]$ (phenomological theory of dielectric relaxation Kremer & Schonals (2003))

$$\frac{\underline{\epsilon}(\omega) - \epsilon_\infty}{\epsilon_s - \epsilon_\infty} = \int_0^\infty \exp(-i\,\omega\,t) \left(-\frac{d\phi(t)}{dt} \right) dt \tag{8}$$

where ϵ_s and ϵ_∞ are are the unrelaxed and relaxed values of the dielectric constant.

3. Resolving the normal mode from the α-relaxation

For low molecular weight, the normal mode of PI overlaps at high frequency with the α-relaxation (Fig. 3). This overlapping is an intrinsic problem in checking the Rouse

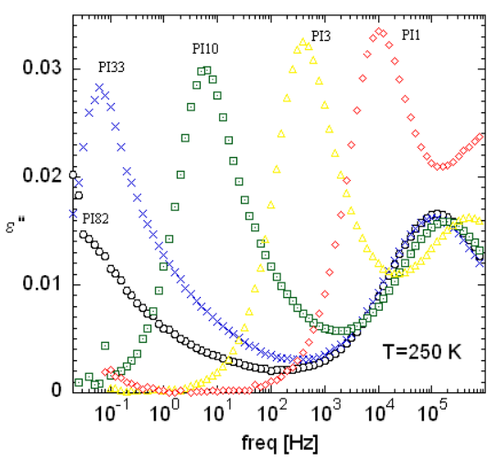

Fig. 3. Dielectric relaxation curves collected at 250 K on PI with different molecular weights.

model (that describes the normal mode dynamics, see next section), since its applicability is limited to chains with moderate molecular weight (below the molecular weight between entanglements). In fact, even by microscopic techniques with spatial resolution as neutron scattering, it is rather difficult to distinguish the border between chain and segmental relaxations Richter et al. (2005).Because the time scale separation between the two dynamical processes is not complete, a detailed analysis of the validity of the Rouse model predictions at high frequencies requires accounting accurately for the α-relaxation contribution.

The imaginary part of the dielectric α-relaxation can be analyzed by using the phenomenological Havriliak-Negami function:

$$\underline{\epsilon}(\omega) = \epsilon_\infty + \frac{\epsilon_s - \epsilon_\infty}{(1 + (i\,\omega\,\tau_{HN})^\alpha)^\gamma}. \tag{9}$$

In addition, a power law contribution ($\propto \omega^{-1}$) was used to account for the normal mode contribution at low frequencies, which is the frequency dependence expected from the Rouse model for frequencies larger than the characteristic one of the shortest mode contribution. Thus, we assumed that the high frequency tail of the normal mode follows a C/ω law and superimposes on the low frequency part of the alpha relaxation losses, being C a free fitting parameter at this stage. The α-relaxation time corresponding to the loss peak maximum was obtained from the parameters of the HN function as follows Kremer & Schonals (2003):

$$\tau_\alpha = \tau_{HN} \frac{\left[sin\left(\frac{\alpha\,\gamma\pi}{2+2\gamma}\right)\right]^{1/\alpha}}{\left[sin\left(\frac{\alpha\,\pi}{2+2\gamma}\right)\right]^{1/\alpha}} \tag{10}$$

The results obtained for samples with different molecular weight at a common temperature of 230 K are shown in Fig. 4. It is evident that in the low molecular weight range the time scale of the segmental dynamics is considerably faster than that corresponding to the high molecular weight limit. This behavior is mainly associated with the plasticizer-like effect of the enchain groups, which are more and more relevant as chain molecular weight decreases. The line in figure 4 describing the experimental behavior for the PI samples investigated is given by:

$$\tau_\alpha(M) = \frac{\tau_\alpha(\infty)}{(1+10000/M)^2} \tag{11}$$

As can be seen in Fig. 3 and 4, the α-relaxation contribution from long chains is nearly

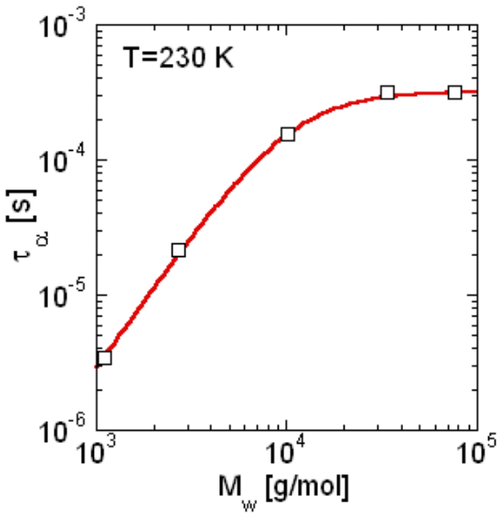

Fig. 4. α-relaxation times of polyisoprene at 230 K as a function of molecular weight. The line corresponds to Eq. 11

independent on molecular mass, but for low molecular masses (c.a. below 20 000 g/mol) it is shifted to higher frequencies and slightly broader. Because the rather small length scale involved in the segmental dynamics (around a nanometer) Cangialosi et al. (2007); Inoue et al. (2002a) it is expected that for a relatively low molecular weight sample, as PI-3, there would be contributions to the α-relaxation with different time scales originated because the presence of chains of different lengths. This could explain the fact that the α-relaxation peak of the PI-3 sample is slightly broader than that of a high molecular weight one, the PI-82 for instance (see Figure 3). Thus, in order to take this small effect into account we decided to describe the α-relaxation of the PI-3 sample as a superposition of different contributions. The contribution to the α-relaxation from a single chain of molecular weight M is assumed to be of the HN type (Eq. 9), with intensity proportional to the number of units (segments) in the chain, i.e. proportional to M. Under this assumption, the whole α-relaxation would be given as follows:

$$\underline{\epsilon}_\alpha(\omega) = \int \frac{\Delta\epsilon(M)}{(1+(i\,\omega\,\tau_{HN})^\beta)^\gamma} g(M)dM \tag{12}$$

$$= \frac{\Delta\epsilon_\alpha}{M_N} \int \frac{M}{(1+(i\,\omega\,\tau_{HN})^\beta)^\gamma} g(M)dM \tag{13}$$

where g(M) is a Gaussian-like distribution introduced to take into account the effects of the actual molecular weight distribution of the sample:

$$g(M) = \frac{1}{\sqrt{2\,\pi\sigma}} \exp\left(-\frac{(M-M_n)^2}{2\sigma^2}\right) \tag{14}$$

$$\sigma = M_n \sqrt{\frac{M_w}{M_n} - 1} \tag{15}$$

g(M)dM is the number density of chains with molecular weight M, $\Delta\epsilon_\alpha$ is the total dielectric strength associated to the α-relaxation, and $1/M_n$ is just a normalization factor. The parameters β and γ in Eq. 13 were taken form the fitting of the α-relaxation losses of a high molecular weight sample, PI-82, (β = 0.71, γ = 0.50), i.e. the shape of each component has been assumed to be that obtained from the experiment in a sample with a high molecular weight and a narrow distribution. For such a sample no differences between the contributions of distinct chains are expected (see Figure 4). Furthermore, note that for this sample the α-relaxation is very well resolved from the normal mode and, therefore, its shape can be accurately characterized. Moreover, according to Eq. 11, the following expression for $\tau_{HN}(M)$ was used, $\tau_{HN}(M)/\tau_{HN}(\infty) = [1 + (10000/M)^2]^{-1}$, where a value of $\tau_{HN}(\infty) = \tau_{HN}(82000)$ is a good approximation. In order to avoid the unphysical asymptotic behavior ($\epsilon'' \propto \omega^\beta$) given by the HN equation at very low frequencies, the physical asymptotic behavior ($\epsilon'' \propto \omega$) was imposed for frequencies two decades lower than that of the peak loss frequency. This cut-off frequency was chosen because is the highest cut-off frequency allowing a good description of the α-relaxation data from the high molecular weight PI samples. The resulting

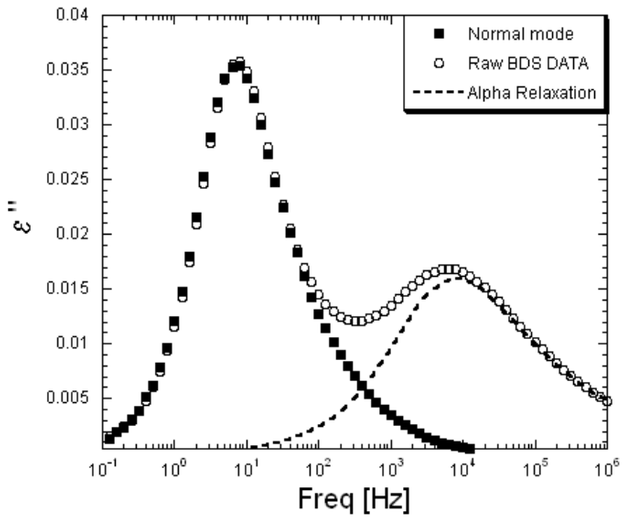

Fig. 5. Resolved normal of PI-3, the dotted line represents the modelled contribution of the α-relaxation. Reprinted with permsision from Riedel et al, Macromolecules 42, 8492-8499 Copyright 2009 American Chemical Society

curve is depicted in Fig. 5 as a dotted line. The value of $\Delta\epsilon_\alpha$ (single adjustable parameter) has been selected to fit the experimental data above f=5e4 Hz, where no appreciable contributions from the normal mode would be expected. After calculating the α-relaxation contribution, the

normal mode contribution can be completely resolved by subtracting it from the experimental data. The so obtained results are depicted in Figure 5 for PI-3.

4. Rouse model: experimental test

The large chain-dynamics of linear polymers is one of the basic and classical problems of polymer physics, and thereby, it has been the subject of intensive investigation, both experimentally and theoretically, over many years Adachi & Kotak (1993); de Gennes (1979); Doi & Edwards (1988); Doxastakis et al. (2003); Hiroshi (2001); McLeish (2002); Watanabe et al. (2002a); Yasuo et al. (1988). Despite of the broad range of models and theoretical approaches existing in the literature there are many aspects of the problem that remain to be understood (see refs.Doi & Edwards (1988); Doxastakis et al. (2003); McLeish (2002); Rouse (1953) and references therein). Most of the current investigations are devoted to the problem of the dynamics of highly entangled polymer melts with different architectures and topologies, and to the rheology of polymer systems of industrial relevance Doi & Edwards (1988); Likhtman & McLeish (2002); Watanabe et al. (n.d.). Concerning the chain-dynamics of unentangled polymers, it is generally assumed that the well-known Rouse model Rouse (1953) provides a suitable theoretical description. The Rouse model represents a linear chain as a series of beds and springs subjected to entropic forces in a medium with a constant friction. Although this simple approach obviously fails in describing the melt dynamics of long chains at longer times, the Rouse model is also used for describing the fastest part of the response of these long chains and thereby it is a common ingredient of all available model and theories. In the past, the validity of the Rouse model has ever been instigated by means of different experimental techniques and also by molecular dynamics simulations. But as already mentioned in the previous section, a full and detailed test of the Rouse model is challenging because in unentangled polymer melts the segmental dynamics (α-relaxation) contributions overlap significantly with the high-frequency components of the chain dynamics. This fact, among others, restricts the use of rheology experiments to test accurately the Rouse model on unentangled polymer chains. It is very hard to obtain rheology data of unentanged polymers in the melt. This is due to the rapid relaxation times of the material and the broad spread of the effect of more local molecular mechanisms that affect the stress relaxation modulus at higher frequencies. We will first detail how we have been able to resolve the normal mode from the α-relaxation in BDS data. Then, we will start our study of the Rouse model by introducing the expression of both complex dielectric permittivity and shear modulus before presenting the full detail of the test of the Rouse model using both rheology and BDS.

4.1 Theory

The random walk is an extremely simple model that accounts quantitatively for many properties of chains and provides the starting point for much of the physics of polymer. In this model, we consider an ideal freely joined chain, made up of N links, each define by a vector $\overrightarrow{r}_i$ and b the average length between the links (Fig. 6). The different links have independent orientations. Thus the path of the polymer in space is a random walk.

The end-to-end vector $\overrightarrow{R}_N(t)$ is the sum of the N jump vectors $\overrightarrow{r}_{i+1} - \overrightarrow{r}_i$ which represent the direction and size of each link in the chain:

$$\overrightarrow{R}_N(t) = \sum_{i=1}^{N-1} \overrightarrow{r}_{i+1} - \overrightarrow{r}_i \tag{16}$$

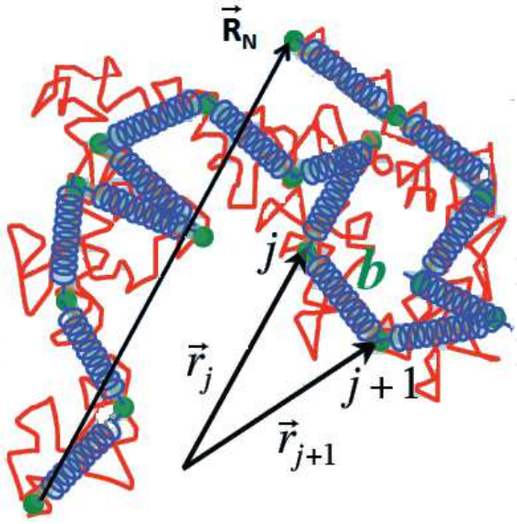

Fig. 6. Schematic representation of the spring model for polymer chain

The mean end-to-end distance is

$$\langle \overrightarrow{R}_N(t)^2 \rangle = N\, b^2 \tag{17}$$

The overall size of a random walk is proportional to the square root of the number of steps.

The correlation function of $\overrightarrow{R}_N(t)$ can be expressed as the sum of the vibration of the so-called Rouse modes:

$$\langle \overrightarrow{R}_N(t)\, \overrightarrow{R}_N(0) \rangle = \frac{2b^2}{N} \sum_{p:odd}^{N-1} cot^2\left(\frac{p\pi}{2N}\right) \exp\left(\frac{-t}{\tau_p}\right) \tag{18}$$

with

$$\tau_p = \frac{\xi b^2}{12\, k_b\, T\, sin^2\left(\frac{p\,\pi}{2N}\right)} \tag{19}$$

In the limit of the long chains, for pπ<2N, we obtain the well known expression of the end-to-end vector:

$$\langle \overrightarrow{R}_N(t)\, \overrightarrow{R}_N(0) \rangle \cong \frac{8\, b^2 N}{\pi^2} \sum_{p:odd} \frac{1}{p^2} \exp\left(-\frac{t}{\tau_p}\right) \tag{20}$$

Due to the factor $1/p^2$ the correlation function of the end-to-end vector is dominated by the slowest mode and as $\tau_p = \frac{\tau_1}{p^2}$ the higher modes are shifted to higher frequencies.

For small deformation, the chain can be approximatively described using a gaussian configuration and the expression of the xy component of the shear stress is given by Doi & Edwards (1988):

$$\sigma_{xy} = \frac{3\,\nu\, k_b T}{N b^2} \sum_{i=1}^{N} \langle (\overrightarrow{r}_{i+1} - \overrightarrow{r}_i)_x (\overrightarrow{r}_{i+1} - \overrightarrow{r}_i)_y \rangle \tag{21}$$

where ν is the number of chain per volume unit.

4.1.1 Expression of $\underline{\epsilon}(\omega)$ in the frame of the Rouse model

BDS measure the time fluctuation of the polarization. Polymers can have dipole moments parallel to the chain backbone, leading to a net "end-to-end" vector. The part of the polarization related with these dipole moments is proportional to the time fluctuation of the end-to-end vector: $\phi(t) = [\overrightarrow{P}(t) \cdot \overrightarrow{P}(0)] \propto [\overrightarrow{R_N}(t) \cdot \overrightarrow{R_N}(0)]$. Using the expression of the end-to-end vector (Eq. 18) in the phenomenological theory of the dielectric relaxation (Eq. 8) we obtain an expression of the frequency dependance of the dielectric permittivity in the frame of the Rouse model:

$$\epsilon'(\omega) \propto \frac{2b^2}{N} \sum_{p:odd}^{N-1} cot^2\left(\frac{p\pi}{2N}\right) \frac{1}{1+\omega^2\tau_p^2} \tag{22}$$

$$\epsilon''(\omega) \propto \frac{2b^2}{N} \sum_{p:odd}^{N-1} cot^2\left(\frac{p\pi}{2N}\right) \frac{\omega\tau_p}{1+\omega^2\tau_p^2} \tag{23}$$

The factor $cot^2(p)$ (which can be developed in $1/p^2$ when p<N) strongly suppress the contribution of high p modes. Therefore, the dielectric permittivity is sensitive to slow (low p modes) and facilitates resolving normal mode and segmental relaxation contributions.

4.1.2 Expression of $\underline{G}(\omega)$ in the frame of the Rouse model

We can calculate the expression of the shear modulus in the time domain from Eq.21, and using a Fourier transform, we obtain:

$$G'(\omega) \propto \sum_{p=1}^{N-1} \frac{\omega^2\tau_p^2/4}{1+\omega^2\tau_p^2/4} \tag{24}$$

$$G''(\omega) \propto \sum_{p=1}^{N-1} \frac{\omega\tau_p/2}{1+\omega^2\tau_p^2/4} \tag{25}$$

All the modes are contributing in the expression of the shear modulus. Therefore, in the case of small chains, rheology is not a convenient experimental technique to resolve the chain modes from the segmental dynamics.

4.2 Test of the Rouse model

4.2.1 Choice of the sample: Working below M_E

The Rouse model describe the dynamics of unentangled polymers only. Therefore it is important to characterize its domains of application. As we will see below, the use of the time temperature superposition (TTS, see next paragraph) to create master curves in rheology is questionable. Figure 7 represents the master plot obtained for PI-82 from different temperatures T=[40, 20, -15, -30, -50]žC (each represented by a different color) shifted to the reference temperature of -50žC. Master curves permits to obtain the full rheology of the polymer. At low frequencies we can see the Maxwell zone ($G' \propto \omega$,$G'' \propto \omega^2$). Then, the elastic plateau, where G'>G", is well defined and the polymer is therefore entangled. After the plateau, the Rouse zone is characterized by $G' \propto G'' \propto \omega^{1/2}$. Rheology allows measuring a value of the molecular weight of entanglement M_E by measuring G_n^0, value of G' at the

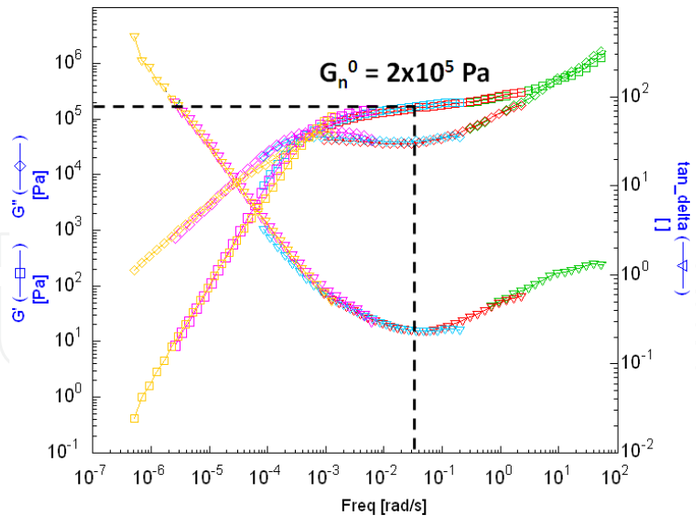

Fig. 7. Master curve of PI-82 at the reference temperature of -50žC

minimum of tan(δ) (around the middle of the elastic plateau). This measurement is made at one temperature, and therefore no master curve is needed to get the value of G_n^0. According to reference Doi & Edwards (1988):

$$M_E = \frac{\rho RT}{G_n^0} \tag{26}$$

where ρ=0.9 g/cm^3 is the density, R = 8.32 J/K/mol is the ideal gas constant and T is the temperature of measurement. Using the value obtained from Fig. 7: $G_n^0 = 2.10^5$ Pa, we obtain a value of M_E=9 kg/mol.

The dielectric normal mode reflects the fluctuations of the end-to-end vector and is dominated by the slowest chain normal mode. As higher modes are scaled and shifted to higher frequencies, the timescale of the normal mode peak, $\tau_N = \frac{2\pi}{f_N}$ (where f_N is the frequency of the maximum of the peak), measured by BDS provides a rather direct access to the Rouse time τ_1 when Rouse theory is fulfilled. Using these values of τ_N at 230 K we have checked whether below the molecular weight between entanglements the Rouse model predictions concerning the molecular weight dependence of the slowest relaxation times ($\tau_1 \propto M^2$) is verified. In Fig. 8 we present the values of the ratio τ_N/τ_α as a function of the molecular mass. The ratio between the longest relaxation time and the value of τ_α obtained at the same temperature in the same experiment is the way used trying to remove the possible variation in τ_N arising from the monomeric friction coefficient, which can be assumed as straightforwardly related with the changes in the glass transition temperature, and hence, with the noticeable effect of end chain groups in the segmental dynamics. Fig. 8 shows that below a molecular weight of around 7 000 g/mol the data scales approximately with M^2. This is just the Rouse model prediction, i.e., what is deduced from Eq. **??** for low-p values where the following approximation holds. This value is intermediate between that of the molecular mass between entanglements (M_e=9 kg/mol) obtained by rheology and that measured from neutron scattering experiments M_e=5 kg/mol Fetters et al. (1994).

Once we have confirmed the range of molecular masses where the molecular weight dependence of the longest relaxation time verifies Eq. **??**, we will test if the whole dielectric

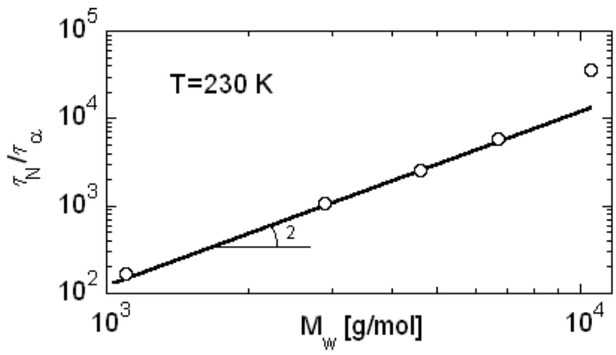

Fig. 8. Ratio τ_N/τ_α , as a function of the molecular weight at 230 K. Solid line represents the behavior predicted by the Rouse model where $\tau_N = \tau_1 \propto M^2$. Reprinted with permsision from Riedel et al, Macromolecules 42, 8492-8499 Copyright 2009 American Chemical Society

normal mode conforms the Rouse model predictions. We have selected the sample PI-3 for this test because, on the one hand, it has a molecular weight sufficiently below of the molecular weight between entanglements (so all the molecular masses of the distribution are below M_E and, on the other hand, it shows a normal mode that is rather well resolved from the segmental α-relaxation contributions to the dielectric losses. Using higher molecular weight samples yield the possibility that the high molecular weight tail of the distribution was above the entanglement molecular weight. On the contrary, for lower molecular weight samples the stronger superposition of the normal mode and the α-relaxation will make the comparison less conclusive (see Fig. 3). For the test, we have taken the data recorded at a temperature of 230 K where the normal mode contribution is completely included within the experimental frequency window, being at the same time the α-relaxation contribution also well captured and then subtracted (see previous section and Figure 5).

4.2.2 Time temperature superposition (TTS)

Figure 9 a shows the high level of accuracy obtained by means of the present BDS experiments when measuring the rather weak dielectric relaxation of a PI-3 sample, for both the normal mode and the α-relaxation. From simple inspection of the data it is apparent that the normal mode peak shifts by changing temperature without any significant change in shape (time temperature superposition is verified for this process), which is one of the predictions of the Rouse model (see eq. 18). However, it is also evident that the shift of the normal mode peak is distinct than that of the α-relaxation one, i.e. the TTS fails for the complete response. **?** This fact is illustrated in Figure 9 b where data at two temperatures where both processes are clearly visible in the frequency window are compared. For this comparison the axes were scaled (by a multiplying factor) in such a way that the normal peaks superimpose. Whereas the superposition in the normal mode range is excellent, the same shift makes the alpha relaxation peak positions to be about half a decade different. The temperature dependance of the normal mode peak can be described by Williams-Landel-Ferry (WLF) Williams et al. (1995) equation:

$$log(a_T) = \frac{C1(T - T_{ref})}{T - T_{ref} + C2} \tag{27}$$

When considering the temperature dependence of the shift factor we found that, whereas for high molecular masses (above that between entanglements) the WLF parameters are the same

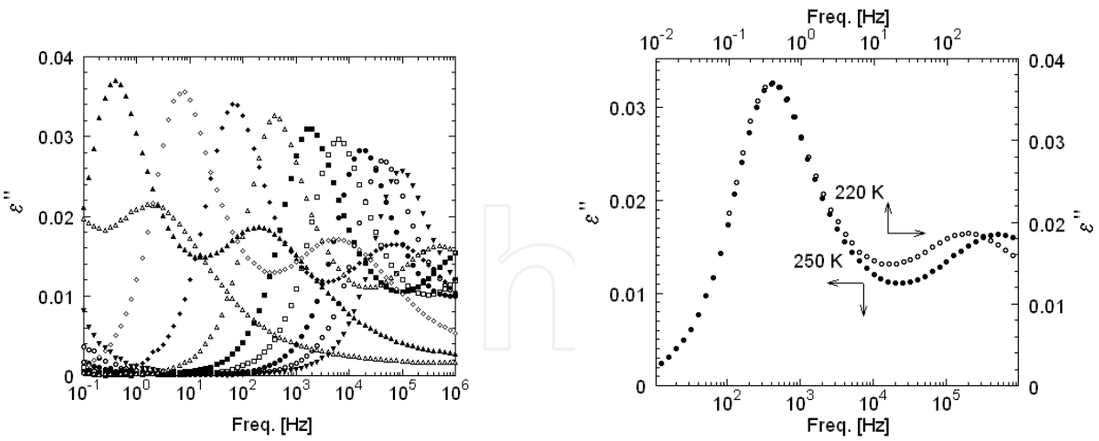

(a) Dielectric spectra of PI3 from 220K (left) to 300K (right) ΔT = 10K.

(b) Comparison of normal mode and α-relaxation frequency shifts for PI3 when temperature is changed from 220 K to 250 K.

Fig. 9. Shift of the dielectric response of PI-3 with temperature. Reprinted with permsision from Riedel et al, Macromolecules 42, 8492-8499 Copyright 2009 American Chemical Society

within uncertainties (WLF parameters with T_g as the reference temperature $C1 = 30.20.7$ and $C2 = 57.00.2K$), for lower molecular weight samples the value of C1 remains the same but C2 becomes noticeably smaller, being 49.2 K for PI-3. This is likely related with the significant variation of Tg in the low molecular range (see Table 1).

The data resulting from the rheology experiments performed on a PI-3 sample of 1.3 mm thickness using two parallel plates of 8 mm diameter are shown in Figure 10. To produce this plot a master curve at a reference temperature T_{ref} = 230 K was built imposing the horizontal shift factor a_T determined from BDS (see above) and a vertical shift factor b_T=T_r/T. Curves have been measured at 215, 220, 225, 230 and 240K, each color represent a temperature. It is apparent that the superposition so obtained is good in the terminal relaxation range, although at the highest frequencies, where the contributions of the segmental dynamics are prominent, the data superposition fails clearly. The use of master curves in rheology experiments is a standard practice because of the rather limited frequency range and the general applicability of the TTS principle to the terminal relaxation range. However, the presence of the segmental dynamics contribution at high frequencies when approaching T_g could make the application of TTS questionable because the different temperature shifts of global and the segmental dynamics (see above). Thus, using rheology data alone the high frequency side of the terminal region could be highly distorted.

4.2.3 Determination of the bead size

To use Eq. 23 we need the previous determination of N, which is not known a priori, as it requires the estimation of the bead size. Adachi and co-workers Adachi et al. (1990) estimated the bead size of PI on the basis of an analysis of the segmental relaxation in terms of a distribution of Debye relaxation times. These authors suggested that a PI bead would contain about 7 monomers. However, a generally accepted approach is to consider that the bead size would be of the order of the Kuhn length, b_k. Inoue et al. (2002b) The literature value of b_k for

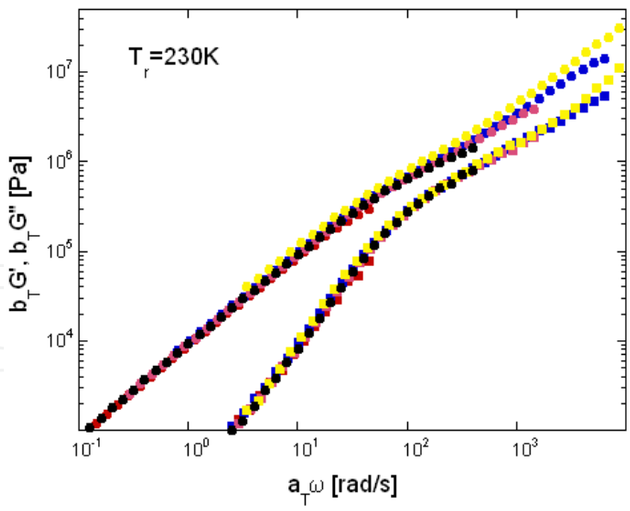

Fig. 10. Rheological master curve of PI-3(reference temperature T_r =230 K) of the real: ■ and imaginary: • parts of the shear modulus.

PI is 0.84 nm,Rubinstein & Colby (2003) which corresponds to a molecular mass of the Kuhn segment of 120 g/mol. This means that a Kuhn segment would contain about 1.5 monomers, about a factor of about 5 less than Adachi et al. estimated. On the other hand, recent results has evidenced that the α-relaxation in the glass transition range probes the polymer segmental motions in a volume comparable to b_k^3. Cangialosi et al. (2007); Lodge & McLeish (2000) Thus, we will introduce a "segmental" Rouse time $\tau_S = \tau_{p=N}$, which apparently have not a clear physical meaning (the fastest Rouse time would be p=N-1) but it can be related with the so-called characteristic Rouse frequency ($W = 3k_bT/b^2$) as $\tau_S^{-1} = 4W$. Nevertheless, τ_S is here used as a convenient parameter for the further analysis. We can identify τ_S at T_g with the α-relaxation time determined at this same temperature, i.e. $\tau_S(Tg)$=5 s. In this way, by using the WLF equation describing the temperature dependence of the normal mode peak, the obtained value of τ_S at 230 K would be 1.1e-4 s. Using this value and that obtained for τ_1 from the normal peak maximum in Eq. **??** a value of N=24 results. Note that according with this value the bead mass would be around 121 g/mol in very good agreement with literature results for the Kuhn segment mass,Rubinstein & Colby (2003) and consequently the corresponding bead size will be nearly identical to b_k.

4.2.4 Monodisperse system

Thus, in order to test the validity of the Rouse model in describing the dielectric normal mode relaxation data we assumed N=24 in Eq. 23, which would be completely predictive, except in an amplitude factor, once the slowest relaxation time τ_1 was determined from the loss peak maximum. The so calculated curve is shown as a dashed line in Figure **??**. It is very clear that the calculated curve is significantly narrower than the experimental data, not only at high frequencies where some overlapping contribution from the α-relaxation could exists, but more importantly also in the low frequency flank of the loss peak. This comparison evidence clearly that the experimental peak is distinctly broader than the calculation of the Rouse model based in Eq. 7, confirming what was already envisaged in Figure 7a of ref. Doxastakis et al. (2003). Nevertheless, an obvious reason for this discrepancy could be the fact that the actual sample has some (small) polydispersity. Despite of the fact that PI samples with a low polydispersity

(1) were chosen, even samples obtained from a very controlled chemistry contains a narrow distribution of the molecular weights, which was not considered in the previous calculation.

4.2.5 Introduction of polydispersity

Now, we are in a situation where it becomes possible to perform a detailed comparison between the experimental normal mode relaxation and the calculated Rouse model expectation. In order to incorporate the small sample polydispersity, the response expected from the Rouse model has been calculated as a weighted superposition of the responses corresponding to chains with different molecular weights. Since the molecular masses of the chains in the PI-3 sample are all below the molecular weight between entanglements, the molecular weight dependence of τ_p will be that given by Eq. 19 for all of the different chains. For calculating $\tau_p(M)$ we have used in Eq. 19 a common value τ_s irrespective of the molecular weight of the particular chain. Furthermore, we calculated $\tau_1(Mw)$ as the reciprocal of the peak angular frequency of the experimental normal mode of this sample.

In this way the Rouse model remains completely predictive and the corresponding dielectric response to be compared with normal mode contribution from the actual sample will be given by:

$$\epsilon''_N(\omega) = \frac{\Delta\epsilon_N}{M_n} \int M \frac{2b^2}{N} \sum_{p:odd}^{N-1} cot^2\left(\frac{p\pi}{2N}\right) g(M) dM \tag{28}$$

where the contribution to the normal mode from a given chain is proportional to the chain dipole moment (to the end-to-end vector), and thus again proportional to M.

As can be seen in Figure 11 (solid line), the sum over all the modes and all the molecular weight provides a satisfactory description of the experimental dielectric losses, namely at frequencies around and above the peak. The excellent agreement evidences that taking into account the (small) polydispersity of the sample under investigation is necessary to provide a good description of the dielectric normal mode contribution by means of the Rouse model, without any adjustable parameter other than the Rouse time, which (for the average molecular mass) is essentially determined from the reciprocal of the maximum loss angular frequency.

4.2.6 BDS and rheology in the same experiment

Once we have found that the Rouse model can account accurately for the chain dynamics as observed by dielectric spectroscopy, the question that arise is if using the very same approach it would be possible to account also for other independent experiments, namely rheology. A key point to perform such a test is to be sure that all the environmental sample conditions remains the same. To be sure about this, we performed simultaneous dielectric and rheology experiments at 230 K. The sample thickness was smaller to balance the data quality of both dielectric and rheological results. We found that a thickness of 0.9 mm using two parallel plates of 25 mm diameter provides a rather good compromise. The output of these experiments at 230 K is shown in Figure 12. Despite of the very different geometry used, the rheological results are in close agreement with those obtained before. In this simultaneous experiment, the dielectric normal mode is clearly resolved so the peak position defining the time scale can be determined with low uncertainty, although again the accuracy of the dielectric relaxation data is not so good as that obtained in the data presented before.

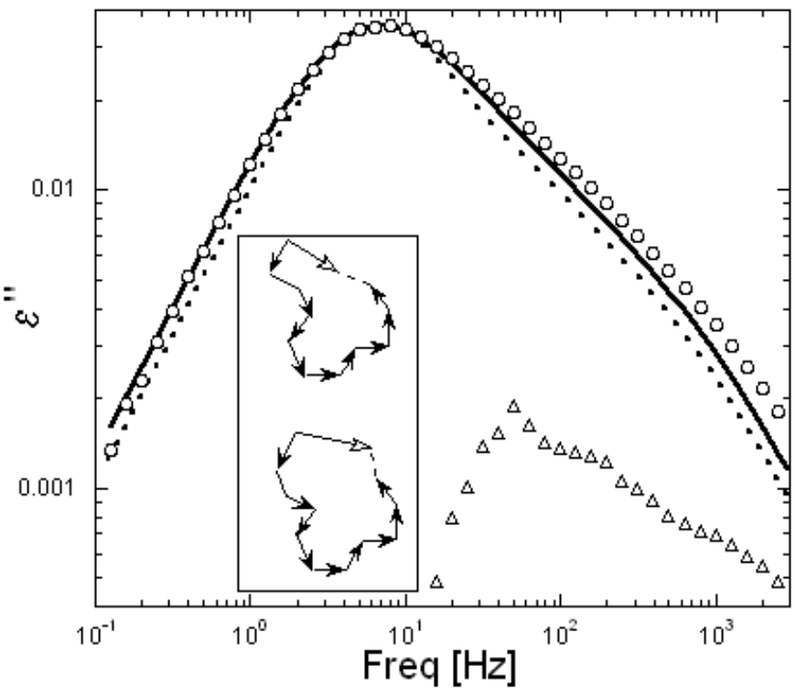

Fig. 11. Resolved normal mode relaxation of PI-3 sample. The lines represent the behaviour predicted by the Rouse model including for the actual sample polydispersity (solid line) and without it (dotted line). Triangles correspond to the difference between the experimental losses and the Rouse model predictions. The inset shows schematically how the presence of configuration defects allows fluctuations of the whole chain dipole moment without variation of the end-to-end vector. Reprinted with permsision from Riedel et al, Macromolecules 42, 8492-8499 Copyright 2009 American Chemical Society

Nevertheless, this experiment will be essential in testing the ability of the Rouse model in accounting simultaneously for both the dielectric and rheology signatures of the whole chain dynamics. The approach used was to determine τ_1 from the dielectric losses, according with the description used above that is able to accurately account for the complete dielectric relaxation spectrum, and to use a similar approach to generate the corresponding rheology behavior. Thus, the only unknown parameter needed to perform the comparison with the experimental G′(ω) and G″(ω) data will be G_∞ (the high frequency limit of the modulus in terminal zone), which in fact it is not needed for calculating tan (δ)= G″(ω)/G′(ω). The equations used were obtained from Eq. RouseRheo1 and RouseRheo2 following the same procedure that the one from BDS:

$$G'(\omega) = \int \frac{G_\infty}{M_n} \sum_{p=1}^{N-1} \frac{\omega^2 \tau_p^2/4}{1+\omega^2 \tau_p^2/4} g(M) dM \tag{29}$$

$$G''(\omega) = \int \frac{G_\infty}{M_n} \sum_{p=1}^{N-1} \frac{\omega \tau_p/2}{1+\omega^2 \tau_p^2/4} g(M) dM \tag{30}$$

The results of the comparison between the calculated responses and the experimental data are shown in Fig. 12. A satisfactory description is obtained for G′(ω) and G″(ω) by means

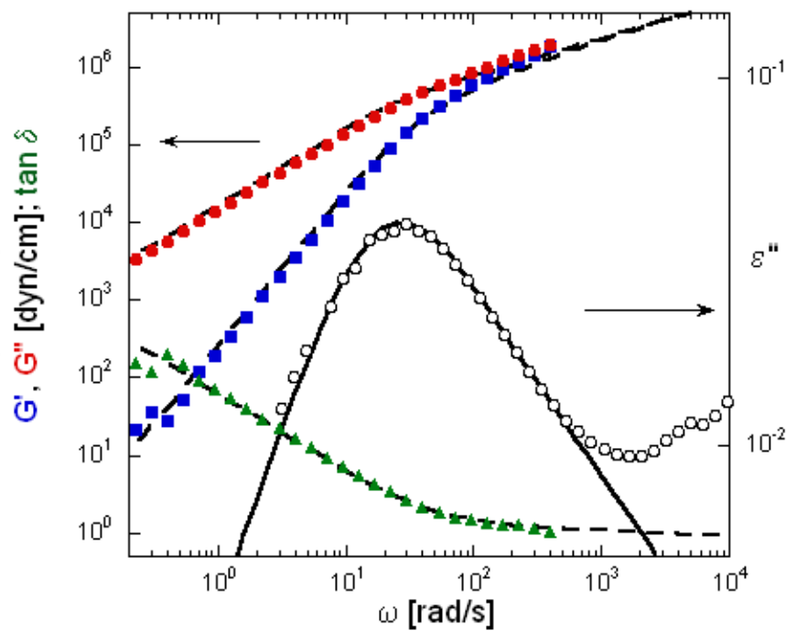

Fig. 12. Simultaneous rheology (G′: ■, G″: ●, tan(δ) : ▲) and BDS experiments (ϵ″: ○) on PI-3 at 230 K. Lines correspond to the description obtained using the Rouse model, with a single set of parameters, for all the data sets.

of the same Rouse model parameters used in describing the dielectric normal mode. More interestingly, the description of tan(δ) is also rather good, for which the previous calculation is compared with the experimental data without any arbitrary scaling. Despite the good agreement obtained, it is worthy of remark that the ability of rheology experiments for checking the Rouse model in full detail is much more limited than the dielectric one because both the narrower frequency range accessible and the stronger overlapping of the segmental dynamics contributions.

4.3 Discussion

Despite the overall good agreement, Figure 11 evidences that the experimental losses are slightly larger (maximum difference about 10%) than the Rouse model prediction in the high frequency side. Although one could consider that this is simply due to the contribution of the overlapping α-relaxation that has not been properly subtracted, the fact that the maximum of these extra losses intensity occurs at frequencies two decades above the segmental relaxation peak (see triangle in Figure 11) seems to point out to other origin. In agreement with this idea, that the frequency distance above the NM peak where the Rouse model description starts underestimating the experimental losses does not depend much on temperature. Thus, extra contributions from some chain-modes are detected in the dielectric normal mode. In fact the peak intensity of the extra losses occurs at the position of the p=3 mode (see triangles in Fig. 11), i.e. the second mode contributing to the dielectric normal mode. All this might evidence the fact that the Rouse model approach ignores several aspects of the actual chain properties as that of the chain stiffness Brodeck et al. (2009) or the lower friction expected to occur at the chain ends Lund et al. (2009). In this context it is noticeable that the contribution from the α-relaxation extended considerably towards the frequency range where the normal mode is

more prominent. In fact the cut-off frequency used for describing the α-relaxation in Fig. 5 was close to 100 Hz, i.e, where the differences between the normal mode response and the Rouse model are more pronounced. This result indicates that for most of the high-p chain modes the segmental relaxation is not completed. This is in contrast to the assumptions of the Rouse model where it is considered that all the internal motions in the chain segment are so fast that their effect can be included in the effective friction coefficient. It is noteworthy that a higher frequency cut-off would be not compatible with the experimental data of the high molecular weight PI samples, and would produce a more prominent underestimation of the dielectric normal mode losses. On the contrary, a lower frequency cut-off would improve slightly the agreement between the normal mode data and the Rouse model prediction but would imply and higher coupling between the segmental dynamics and the whole chain motion. Small deviations from the Rouse model predictions have also been reported from numerical simulations, molecular dynamics calculations and detected by neutron scattering experiments, Brodeck et al. (2009); Doxastakis et al. (2003); Logotheti & Theodorou (2007); Richter et al. (1999) although these deviations become evident only for relatively high p-values. Note, that dielectric experiments being mainly sensitive to the low-p modes can hardly detect such deviations. On the other hand, experiments in solution have also evidenced differences between the experimental data and the predictions of the Rouse model,Watanabe et al. (1995) which were tentatively attributed to chain overlapping effects since the deviations occur above a given concentration. Nonetheless, there are also possible experimental sources for the small extra high frequency contributions to the dielectric losses as it would be the presence in the actual polymer of a fraction of monomeric units others than the 1,4-cis ones (up to 20%). The motion of such units, having a much smaller component of the dipole moment parallel to the chain contour, would produce small amplitude fluctuations of the whole dipole moment uncorrelated with the fluctuations of the end-to-end vector (see inset in Figure 11). The chain motions around these 'configuration defects' would generate a relatively weak and fast contribution to the dielectric normal mode that could explain the experimental data. Unfortunately, the actual sample microstructure prevents to definitively address whether the deviations from the Rouse model predictions are actually indicative of its limitations.

5. Dynamics regimes as a function of the molecular weight and effects of entanglement

As shown in the previous section, the polymer dynamics follows different regimes as a function of the molecular weight and molecular weight distribution. Abdel-Goad et al Abdel-Goad et al. (2004), using rheology measurements coupled with an empirical Winter-relaxation BSW-model obtained three different exponents (1, 3.4 and 3) in the molecular weight dependence of the zero shear viscosity. Previous BDS studies on the molecular weight dependence of the normal mode relaxation time showed a crossover from the unentangled dynamics to the entanglement regime Adachi & Kotak (1993); Boese & Kremer (1990); Hiroshi (2001;?); Yasuo et al. (1988). The reptational tube model was first introduced by de Gennes de Gennes (1979) and developed by Doi and Edwads Doi & Edwards (1988) to described this phenomena of entanglement. Many corrections (as Contour Length Fluctuation or Constraints Release) have been added to the pure reptation in order to reach a totally predictive theory McLeish (2002); Viovy et al. (2002). However, none of BDS experiment has been able to access the crossover to exponent 3 expected by the pure reptation theory which, as aforementioned, has been detected for the viscosity. In this section, we will detail how careful BDS experiments allow detecting the two different crossovers from

the Rouse up to the pure reptation regime. Entanglement effects in BDS spectra will be also analyzed. Finally, the possible influence of the narrow molecular weight distribution of the samples on the dielectric loss shape will be discussed.

5.1 Low molecular weight

As can be seen in Fig. 3 the fast variation of the normal mode relaxation peak prevents detecting it in the frequency window at 250K for molecular weight higher than 80 kg/mol. Thus, we will first focus the analysis on the samples with lower molecular weight. As already mentioned, for low molecular masses the changes in the local friction coefficient (arising because the significant changes in the end chain groups accompanying the changes in molecular weight) influences the relaxation time. Therefore, just as in Fig. 8, the ratio of the normal mode time scale to that of the α-relaxation was evaluated (Fig. 13). To increase the plot

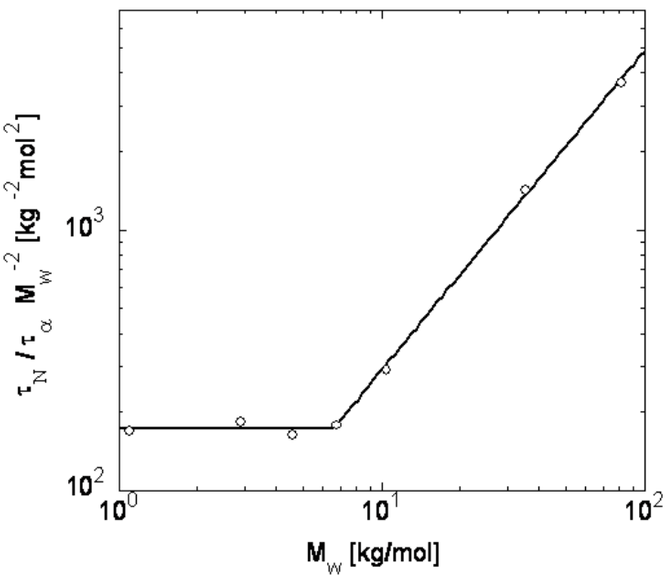

Fig. 13. Longest and segmental relaxation time ratio as a function of the molecular weight at 250 K. The vertical axis is scaled by M^2 to emphasize the transition from the Rouse to the intermediate regime. The solid line corresponds to the description of the data with a sharp crossover between two power law regimes with different exponents. Reprinted with permsision from Riedel et al, Rheologica Acta 49, 507-512 Copyright 2010 Springer

sensitivity to changes between the different regimes a factor of M_w^{-2} has been applied to the ratio between the characteristic times (reciprocal of the peak angular frequency) of the two relaxation processes. As already mentioned, the M_w^2 dependence expected for unentangled polymers on the basis of the Rouse theory is fulfilled for samples with molecular weight below 7 kg/mol. The exponent describing the higher molecular mass range considered in this plot was 3.20.1 which is distinctly lower, but close, to the 3.4 usually found in rheological experiments Ferry (1995). It is noteworthy that imposing this exponent to fit our data will result in a higher value of the crossover molecular weight, thus increasing the discrepancy with the reported/admitted value of M_e=5kg/mol measured by neutron scattering Fetters et al. (1994). It is noteworthy that, as it is well know, the ratio τ_N/τ_α will change with temperature Ding & Sokolov (2006). Nevertheless, the previous results will not change

significantly using data at other temperatures because the changes in the value τ_N/τ_α will be very similar for all the samples having different molecular weights and, consequently, the resulting molecular weight dependence would be unaltered.

5.2 High molecular weight

After analyzing the molecular weight dependence of the end-to-end fluctuations in the low and moderate molecular weight range, now we will focus the attention in the highest accessible molecular weights. In the high molecular weight range, the comparison among the different samples has to be performed at a significantly higher temperature due to the dramatic slowing down of the chain dynamics. The more suitable temperatures are those where the normal mode loss peak of the sample with the highest molecular weight occurs in the low frequency range of the experimental window. An additional factor that have to be taken into account is the fact that by increasing temperature the conductivity contribution to the dielectric losses becomes more prominent. The conductivity contribution appears as a ω^{-1} increasing of the dielectric losses. This is an important issue even for high quality samples when the experiments require accessing to the low frequencies at temperatures far above T_g. This situation is illustrated in Fig. 14 for the raw data of the PI sample having the highest investigated molecular weight. It is apparent that at 340 K the normal mode

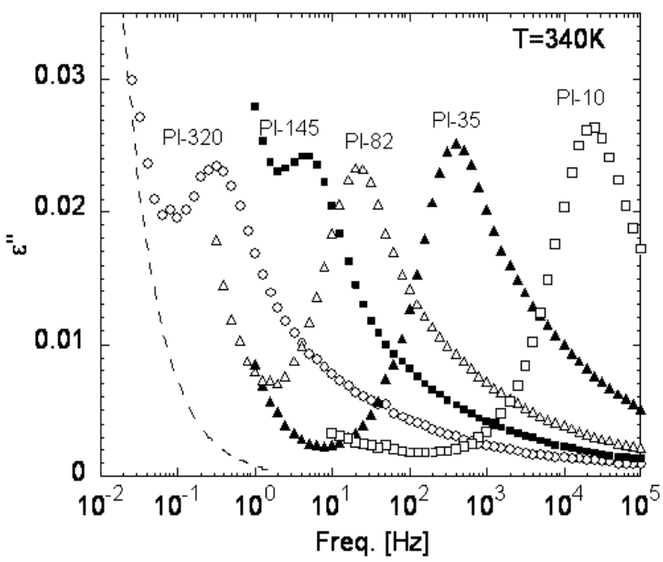

Fig. 14. Normal mode of the high molecular weight PI samples. Dashed line represents the calculated conductivity contribution to the dielectric losses for the PI-320 sample. Reprinted with permsision from Riedel et al, Rheologica Acta 49, 507-512 Copyright 2010 Springer

peak can be well resolved from conductivity for this sample but it would be hard to resolve the normal mode relaxation at this temperature for a sample with a significantly higher molecular weight. Furthermore, increasing temperature would not improve the situation since the overlapping of the conductivity contribution with the normal mode relaxation will also increase. This is a serious limitation of the dielectric methods for investigating the slowest chain dynamics in highly entangled systems. Nevertheless, as shown in Fig. 14, resolving the normal mode peak was possible for all the samples investigated although the contribution from conductivity will increase the uncertainty in the peak position for the samples with very

high molecular weight. Figure 15 shows the molecular weight dependence of the slowest relaxation time for the high molecular weight regime obtained from the data presented in Fig. 14. Trying to increase the sensitivity of the plot to possible changes in behavior the data

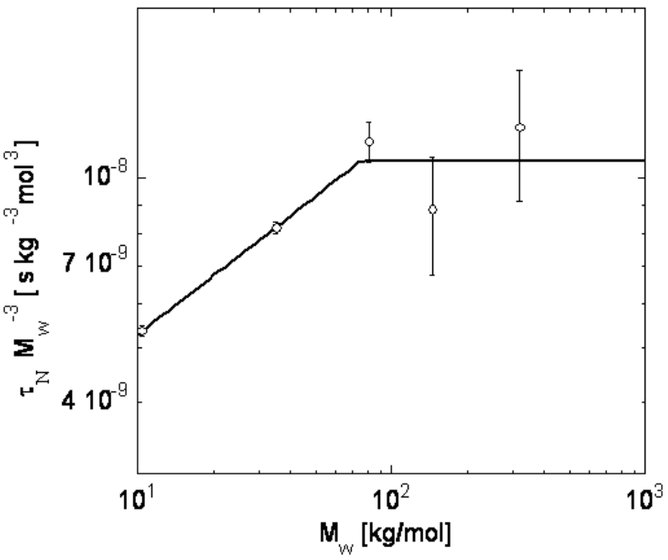

Fig. 15. Longest relaxation time from the higher molecular weight PI samples. The graph is scaled to M^3 to emphasize the crossover from the intermediate to the reptation regime. The solid line corresponds to the description of the data with a sharp crossover between to power law regimes with different exponents. Reprinted with permsision from Riedel et al, Rheologica Acta 49, 507-512 Copyright 2010 Springer

have been multiplied by M_w^{-3}, which would produce a molecular weight independent result for a pure reptation regime. Despite of the uncertainties involved, our results evidence that for the highest molecular weight samples the molecular mass dependence approach the pure reptation regime expectation. The line in Fig. 4 corresponds to a crossover from and exponent 3.35 to a pure reptation-like regime. The small difference between this exponent and that obtained above from Figure 2 is more likely due to the fact that the sample with the lower molecular weight considered in Fig. 4 have a significantly lower glass transition temperature, an effect not been considered in Fig. 4. The crossover molecular weight obtained from Fig. 4 is 7510 kg/mol, i.e. it corresponds to about 15 times M_e. This value is slightly lower than that determined from viscosity data Abdel-Goad et al. (2004).

5.3 Discussion

The results previously described showed three different regimes for the molecular weight dependence of the chain longest relaxation time in PI, one below 7 kg/mol following the Rouse model prediction as expected for a non-entangled polymer melts, other above 75 kg/mol where the reptation theory provides a good description and an intermediate one, where the polymer is entangled but other mechanisms (like contour length fluctuations or constraints release) in addition to reptation would control the whole chain dynamics. In the rheological experiments above referred Abdel-Goad et al. (2004) it was shown that the viscosity of high molecular weight PI samples conforms well the reptation theory predictions.

Thus, we decided to test up to what extent the pure reptation theory is able to describe the normal mode relaxation spectrum of the highly entangled PI samples. This test can evidence the ability of the reptation theory to capture the main features of the slowest chain dynamics, despite the well documented failure of the reptation theory in accounting for the whole chain dynamics, even in the high molecular weight range. This is clearly evidenced by the reported mismatching of the normalized dielectric and rheological spectra Watanabe et al. (2002b). To this end, we compared our experimental data on the high molecular mass samples with the corresponding reptation theory predictions for the dielectric permittivity. This relation is similar to the one obtained in the frame of the Rouse model (Eq. 23. As the chain are long, N>p and the cot^2 can be developed in $1/p^2$. The value of $\tau_p = \tau_1/p^2$ is replaced by τ_d/p^2 where τ_d is the disentanglement time (reptation) time, which would correspond in good approximation to τ_N.

$$\epsilon''(\omega) \propto \sum_{p:odd}^{N-1} \frac{1}{p^2} \frac{\omega\,\tau_d/p^2}{1+(\omega^2\,\tau_d/p^2)^2} \tag{31}$$

Figure 16 shows the direct comparison between the experimental data for some of the samples investigated (symbols) having all of them the lowest available polydispersity index (1.05) and the pure reptation theory prediction (solid line). Both vertical and horizontal scaling factors have been applied to obtain a good matching of the peaks. It should be noted that the possible conductivity contributions to the normal mode relaxation were subtracted. The inset shows separately the data of the highest molecular weight sample because it has a markedly broader molecular weight distribution (polydispersity index 1.14). From Fig. 16 it becomes apparent

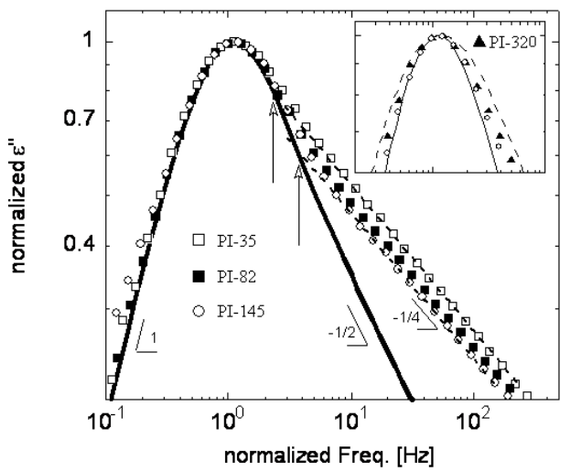

Fig. 16. Comparison of the BDS data of high molecular weight (symbols) with pure reptation theory (solid line). Dashed straight line showing the ij power law behavior of the samples with PI-33 and PI-145 are also shown. The vertical arrows indicate the crossover frequency between both regimes. The inset presents for comparison the highest molecular weight data (PI-320) with a high polydispersity (1.14) with that of smaller polydispersity (1.04). The dashed line represents what would be the reptation theory expectation when a very crude approximation is used to account the effect of the molecular weight. Reprinted with permsision from Riedel et al, Rheologica Acta 49, 507-512 Copyright 2010 Springer

that in the high frequency side of the loss peak deviations from the reptation predictions on

the end-to-end vector fluctuations persist even for the highest molecular weight investigated. Whereas the high frequency behavior expected from the reptation theory is a power law with exponent -1/2, the experimental data present and exponent -1/4 (see Figure 16), which would be a signature of the relevance of chain contour length fluctuations at least in this high frequency side of the normal mode relaxation. Nevertheless, it is also clear that the range of these deviations reduce when increasing molecular weight. The vertical arrows in Fig. 5 shows that a factor of 5 increasing in molecular weight makes the crossover frequency to increase in a factor of about 2. By inspection of the rheological data reported by Abdel-Goad et al, Abdel-Goad et al. (2004) it is also apparent that in the very high molecular weight range where the viscosity scales as predicted by reptation theory the terminal relaxation is far from being properly described by this theory. Eventually the normal mode description by the pure reptation theory could be obtained only at extremely higher molecular weights, for which, as aforementioned, the dielectric experiments will not be suitable for investigating the extremely slow chain dynamics. Concerning this, it has been shown McLeish (2002) that for polyethylene de frequency dependence of the loss shear modulus verifies the reptation prediction only for a molecular weight as high as of 800 kg/mol, which for this polymer corresponds to about 400 times M_e, i.e., it would correspond to about 3000 kg/mol for PI. Taking the above-calculated shift of the crossover frequency into account, for this limiting molecular weight the crossover frequency would occur at around 20 Hz and the failure of the repetition theory description would be hardly detectable by using the same scale as in Figure 16. Figure 16 also shows that both the maximum and the low frequency side of the loss peak is well accounted by the reptation theory without any evident deviation, except for the sample having a broader distribution of molecular weight, which shows a distinctly broader normal mode peak (see inset of Fig. 16). This comparison evidences that the molecular weight distribution have a noticeable effect on the normal mode spectrum shape. We remind that the effect of the molecular weight distribution on the normal mode was properly accounted for in an unentangled PI sample by assuming that the contributions from chains in the sample with distinct molecular weight simply superimpose (see previous section on the Rouse model). When we tried the same approach with the higher molecular weight samples (dashed line in the inset of Fig. 16) it becomes evident that the situation for well-entangled polymers is different. Even by using the smallest polydispersity (1.04) the calculated response overestimates by far the broadening of the peak for the sample with highest polydispersity (1.14). Thus, for highly entangled polymers the effect of the molecular weight distribution on the normal mode is less evident than that observed in the unentangled polymer case. In fact, the complete disentanglement of a chain involves also the motions of the chains around, which would have a different molecular weight, being therefore the resulting time scale some kind of average of those corresponding to the ideally monodisperse melts. As a result the longest relaxation time in highly entangled melts should not dependent greatly on the molecular weight distribution provided it is not very broad.

6. Conclusion

In this chapter, we have used broadband dielectric spectroscopy (BDS) and rheology to study properties of linear polymers. We have focused our study on the large chain dynamics (normal mode), described by the reptational tube theory and the Rouse model when the polymer is entangled or not, respectively.

By means of broad-band dielectric spectroscopy we have resolved the normal mode relaxation of a non-entangled 1,4-cis-poly(isoprene) (PI) and therefore accessed to the end-to-end vector dynamics over a broad frequency/time range. A remarkably good comparison of the data with the Rouse model predictions is found if the effect of the actual narrow distribution of molecular masses of the sample investigated is accounted. The very same approach was found to provide a good description of a simultaneous dielectric/rheology experiment. The small excess contributions found in the high frequency side of the experimental dielectric normal mode losses could be associated, at least partially, to the sample microstructure details. Therefore, we conclude that the Rouse model accounts within experimental uncertainties for the end-to-end dynamics of unentangled PI, once the molecular weight distribution effects are considered. A more sensitive test would require an unentangled nearly monodisperse full 1,4-cis-polyisoprene sample, which can hardly be available.

Further experiments have permitted to detect two crossovers in the molecular weight dependence of the end-to-end relaxation time. The first corresponds to the crossover from the range where the Rouse theory is applicable to the entangled limited range, being the crossover molecular weight 6.5 $\pm$ 0.5 kg/mol, i.e. slightly above the molecular weight between entanglements. The crossover from the intermediate range to the behavior predicted by the pure reptation theory is found at around 75 $\pm$ 10 kg/mol, which corresponds to 15 times the molecular weight between entanglements. Despite of the fact that the reptation theory is able to describe the molecular weight dependence of the slowest relaxation time for these high molecular weight samples, the shape of the normal mode spectrum is still markedly different from that expected by this theory. Eventually, only at a much higher molecular weight (hundred times the molecular weight between entanglements) the reptation theory could completely describe the normal mode relaxation associate to the chain dynamics. Unfortunately, dielectric experiments in this range are not feasible.

To conclude, in this chapter we have shown that dielectric spectroscopy and rheology permitted to obtain physical information about polymer. Even if these two techniques measure different properties, the origin of these properties, is the same: the dynamics. As they permit to extend our knowledge on polymer dynamics, these techniques will allow a better understanding and control of polymer properties.

7. References

Abdel-Goad, M., Pyckhout-Hintzen, W., Kahle, S., Allgaier, J., Richter, D. & Fetters, L. J. (2004). Rheological properties of 1,4-polyisoprene over a large molecular weight range, *Macromolecules* 37(21): 8135–8144.

Adachi, K. & Kotak (1993). Dielectric normal mode relaxation, *Progress in polymer science* 18(3): 585.

Adachi, K., Yoshida, H., Fukui, F. & Kotaka, T. (1990). Comparison of dielectric and viscoelastic relaxation spectra of polyisoprene, *Macromolecules* 23(12): 3138–3144. doi: 10.1021/ma00214a018.

Boese, D. & Kremer, F. (1990). Molecular dynamics in bulk cis-polyisoprene as studied by dielectric spectroscopy, *Macromolecules* 23(3): 829–835.

Brodeck, M., Alvarez, F., Arbe, A., Juranyi, F., Unruh, T., Holderer, O., Colmenero, J. & Richter, D. (2009). Study of the dynamics of poly(ethylene oxide) by combining molecular dynamic simulations and neutron scattering experiments, *The Journal of Chemical Physics* 130(9): 094908.

Cangialosi, D., Alegria, A. & Colmenero, J. (2007). Route to calculate the length scale for the glass transition in polymers, *Physical Review E* 76(1): 011514. Copyright (C) 2010 The American Physical Society Please report any problems to prola@aps.org PRE.

de Gennes, P. G. (1979). *Scaling Concepts in Polymer Physics*, Cornell University Press, Ithaca and London.

Ding, Y. & Sokolov, A. P. (2006). Breakdown of time temperature superposition principle and universality of chain dynamics in polymers, *Macromolecules* 39(9): 3322–3326.

Doi, M. & Edwards, S. F. (1988). *The theory of polymer dynamics*, Clarendon, Oxford.

Doxastakis, M., Theodorou, D. N., Fytas, G., Kremer, F., Faller, R., Muller-Plathe, F. & Hadjichristidis, N. (2003). Chain and local dynamics of polyisoprene as probed by experiments and computer simulations, *The Journal of Chemical Physics* 119(13): 6883–6894.

Ferry, J. D. (1995). *Viscoelastic Properties of Polymers*, Oxford University Press, New York.

Fetters, L. J., Lohse, D. J., Richter, D., Witten, T. A. & Zirkel, A. (1994). Connection between polymer molecular weight, density, chain dimensions, and melt viscoelastic properties, *Macromolecules* 27(17): 4639–4647. doi: 10.1021/ma00095a001.

Hiroshi, W. (2001). Dielectric relaxation of type-a polymers in melts and solutions, *Macromolecular Rapid Communications* 22(3): 127–175. 10.1002/1521-3927(200102) 22:3 <127::AID-MARC127>3.0.CO;2-S.

Inoue, T., Uematsu, T. & Osaki, K. (2002a). The significance of the rouse segment: Its concentration dependence, *Macromolecules* 35(3): 820–826. doi: 10.1021/ma011037m.

Inoue, T., Uematsu, T. & Osaki, K. (2002b). The significance of the rouse segment: Its concentration dependence, *Macromolecules* 35(3): 820–826. doi: 10.1021/ma011037m.

Kremer, F. & Schonals, A. (2003). *Broadband Dielectric Spectroscopy*, Springer, Berlin.

Likhtman, A. E. & McLeish, T. C. B. (2002). Quantitative theory for linear dynamics of linear entangled polymers, *Macromolecules* 35(16): 6332–6343. doi: 10.1021/ma0200219.

Lodge, T. P. & McLeish, T. C. B. (2000). Self-concentrations and effective glass transition temperatures in polymer blends, *Macromolecules* 33(14): 5278–5284. doi: 10.1021/ma9921706.

Logotheti, G. E. & Theodorou, D. N. (2007). Segmental and chain dynamics of isotactic polypropylene melts, *Macromolecules* 40(6): 2235–2245. doi: 10.1021/ma062234u.

Lund, R., Plaza-Garcia, S., Alegria, A., Colmenero, J., Janoski, J., Chowdhury, S. R. & Quirk, R. P. (2009). Polymer dynamics of well-defined, chain-end-functionalized polystyrenes by dielectric spectroscopy, *Macromolecules* 42(22): 8875–8881. doi: 10.1021/ma901617u.

McLeish, T. C. B. (2002). Tube theory of entangled polymer dynamics, *Advances in Physics* 51(6): 1379.

Richter, D., M.Monkenbusch, Arbe, A. & Colmenero, J. (2005). *Neutron Spin Echo in Polymer Systems*, Springer, Berlin.

Richter, D., Monkenbusch, M., Allgeier, J., Arbe, A., Colmenero, J., Farago, B., Bae, Y. C. & Faust, R. (1999). From rouse dynamics to local relaxation: A neutron spin echo study on polyisobutylene melts, *The Journal of Chemical Physics* 111(13): 6107–6120.

Rouse, P. E. (1953). A theory for the linear elasticity properties of dilute solutions of coiling polymers, *The Journal of Chemical Physics* 21(7).

Rubinstein, M. & Colby, R. H. (2003). *Polymer Physics*, Oxford University, New York.

Stockmayer, W. (1967). Dielectric disperson in solutions of flexible polymers, *Pure Applied Chemesitry* p. 539.

Viovy, J. L., Rubinstein, M. & Colby, R. H. (2002). Constraint release in polymer melts: tube reorganization versus tube dilation, *Macromolecules* 24(12): 3587–3596. doi: 10.1021/ma00012a020.

Watanabe, H., Matsumiya, Y. & Inoue, T. (2002a). Dielectric and viscoelastic relaxation of highly entangled star polyisoprene: Quantitative test of tube dilation model, *Macromolecules* 35(6): 2339–2357. doi: 10.1021/ma011782z.

Watanabe, H., Matsumiya, Y. & Inoue, T. (2002b). Dielectric and viscoelastic relaxation of highly entangled star polyisoprene: Quantitative test of tube dilation model, *Macromolecules* 35(6): 2339–2357. doi: 10.1021/ma011782z.

Watanabe, H., Sawada, T. & Matsumiya, Y. (n.d.). Constraint release in star/star blends and partial tube dilation in monodisperse star systems, *Macromolecules* 39(7): 2553–2561. doi: 10.1021/ma0600198.

Watanabe, H., Yamada, H. & Urakawa, O. (1995). Dielectric relaxation of dipole-inverted cis-polyisoprene solutions, *Macromolecules* 28(19): 6443–6453. doi: 10.1021/ma00 123a009.

Williams, M. L., Landel, R. F. & Ferry, J. D. (1995). Mechanical properties of substances of high molecular weight in amorphous polymers and other glass-forming liquids, *Journal of American Chemical Society* 77(19): 3701–3707.

Yasuo, I., Keiichiro, A. & Tadao, K. (1988). Further investigation of the dielectric normal mode process in undiluted cis-polyisoprene with narrow distribution of molecular weight, *The Journal of Chemical Physics* 89(12): 7585–7592.

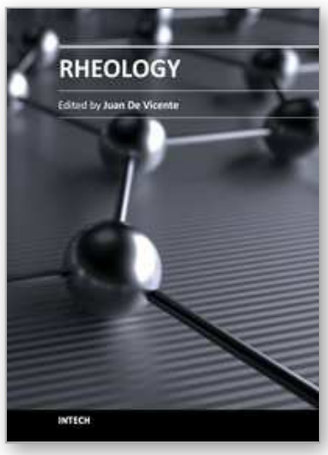

Rheology

Edited by Dr. Juan De Vicente

ISBN 978-953-51-0187-1
Hard cover, 350 pages
Publisher InTech
Published online 07, March, 2012
Published in print edition March, 2012

This book contains a wealth of useful information on current rheology research. By covering a broad variety of rheology-related topics, this e-book is addressed to a wide spectrum of academic and applied researchers and scientists but it could also prove useful to industry specialists. The subject areas include, polymer gels, food rheology, drilling fluids and liquid crystals among others.

How to reference

In order to correctly reference this scholarly work, feel free to copy and paste the following:

Clement Riedel, Angel Alegria, Juan Colmenero and Phillipe Tordjeman (2012). Polymer Rheology by Dielectric Spectroscopy, Rheology, Dr. Juan De Vicente (Ed.), ISBN: 978-953-51-0187-1, InTech, Available from: http://www.intechopen.com/books/rheology/polymer-rheology-by-dielectric-spectroscopy

INTECH
open science | open minds

InTech Europe
University Campus STeP Ri
Slavka Krautzeka 83/A
51000 Rijeka, Croatia
Phone: +385 (51) 770 447
Fax: +385 (51) 686 166
www.intechopen.com

InTech China
Unit 405, Office Block, Hotel Equatorial Shanghai
No.65, Yan An Road (West), Shanghai, 200040, China
中国上海市延安西路65号上海国际贵都大饭店办公楼405单元
Phone: +86-21-62489820
Fax: +86-21-62489821

IntechOpen